P- ISSN 1991-8941 E-ISSN 2706-6703
2024,(18), (02):112 – 122

Journal of University of Anbar for Pure Science (JUAPS)

Open Access

Preparing sulfur nanoparticles and determining their effect on the photodegradation of polycarbonates

Rand Malallah Hassan* , Hameed Khalid Ali , Muthana Mohammad Sirhan

Department of Chemistry, College of Education for Pure Science , University Of Anbar, Ramadi, Iraq;

ARTICLE INFO

Received: 22 / 03 /2024
Accepted: 30/ 06 /2024
Available online: 31/ 12 /2024

10.37652/juaps.2024.148119.1223

Keywords:
polycarbonate, Photodissociation, nano, sulfur , Polymers

Abstract

This study involved the preparation of sulfur nanoparticles using the extract of *Ziziphus spina* leaves and examined their effect on the photodegradation of polycarbonate membranes with a thickness of 60±5 microns, after adding various concentrations of the nano additive (0.1%, 0.05%, 0.025%, 0.0125%, and 0.00625%) to a polycarbonate solution dissolved in chloroform. Sulfur nanoparticles were characterized using different techniques such as SEM, XRD, and FT-IR. A band at 460 cm^{-1} was identified according to FT-IR analysis, indicating the formation of sulfur nanoparticles. Photodegradation of polycarbonates, with and without the additive, was monitored by UV-visible analysis at 356 nm over varying irradiation times (0, 30, 60, 120, and 180 h), calculating the rate constant of photolytic fragmentation for the polymer additive. Results showed an increase in the photodegradation of polymer films with an increase in the concentration of the nanomaterial compared with films without the additive. Using FT-IR analysis, the carbonyl absorption coefficient was calculated and found to increase with the concentration of the added nanosulfur, consistent with the Kd values (rate constant of photolytic fragmentation). Additionally, the average molecular weight of the polymer, the degree of disintegration, and the numerical rate of polymer chain scission were calculated by using a viscometer. We observed that the average molecular weight of the polymer decreased with increasing irradiation time and increasing rate of chain scission.

1. INTRODUCTION

Large molecules known as polymers are created by linking many small molecules or monomers together. Polymerization is the process of linking monomers to form polymers [1]. Many industries, including packaging, construction, and medical applications, rely heavily on polymers [2]. Polycarbonate (PC) is an important engineering plastic that finds extensive application due to its high transparency, durability, and versatility [3]. A few examples include transparent sheets for greenhouses, optical media such as CDs, and electrical and electronic devices like computers and smartphones. It is also utilized in industries such as automotive, medical equipment,
packaging, entertainment, bottles, safety products, and health care. PC is one of the thermoplastic polymers [4]. Polycarbonate is often used as a stronger, lighter alternative to metals in items such as roofing and glass because it is lightweight and has good electrical qualities. When phosgene reacts with bisphenol A, polycarbonate is produced [5].

Every type of polymer (natural, synthetic, and semi-synthetic) is susceptible to photorefraction, especially when exposed to intense ultraviolet (UV) radiation, which causes the changing in mechanical, physical, and chemical features of material with turning to yellowish color [6], The physical and chemical changes resulting from exposing polymers to ultraviolet or visible light are known as light-induced polymer degradation, or photodegradation [7]. In order to understand the chemical changing, physical changing and the relationship between them in polycarbonate and how to influence the overall performance of the material, the research is interested in studying the effects of ultraviolet radiation on this process [8].

One contemporary technology used in many industries, including agriculture, is nanotechnology [9]. “Dwarf” is the ancient Greek word for very small, and is the source of the prefix “nano”. Tiny substance technology is another definition of nanomaterials which can be considered among the sciences and engineering of reproducible substances [10].

Although nanomaterials are dwarf; However, its applications in life are wide, most notably industrial, electronic, solar energy, and medical fields. These are

*Corresponding author at : Department of Chemistry, College of Education for Pure Science , University Of Anbar, Ramadi, Iraq
ORCID:https:// https://orcid.org/0000-0000-0000-0000 ,
Tel: +964 7000000000
Email: ran21u4011@uoanbar.edu.iq

unique properties for materials ranging in size from 1-100 nanometers [11]. Sulfur (S) nonmetallic chemical element (atomic number 16). It is one of the necessary elements for the life of living organisms, especially plants. Problems such as low yields, poor nutritional value, and greater exposure to diseases can affect the plant due to sulfur deficiency [12]. Various fields, such as the manufacture of vegetable fertilizers, pesticides, fumigation, antimicrobials, medical and healing fields, the textile and rubber industry, and biofiltration processes, can all contribute significantly by sulfur. Sulfur nanoparticles are of great benefit in pharmaceutical development and modification of carbon nanotubes [13]. This study used Ziziphus-spina tree leaves to produce sulfur nanoparticles (SNPS) in an environmentally friendly manner. To increase the value of photodegradation of polymer (polycarbonate); nanoscale sulfur can be used as a catalyst. Variety methods was used to study the mechanism of polymer degradation, including UV-visible and infrared radiation. Use a red viscometer and check the rate of change of molecular weight.

2. MATERIALS AND METHODS

Plant extraction

Samples were obtained from the leaves of *Z. spina* trees and washed with running water and distilled water. After being left to dry in the shade, the leaves were crushed in a mortar to produce a powder of the same size. The powder was then kept in the shade after being sifted to remove any particles stuck to it. A 500 mL glass jar was filled with 20 g of *Z. spina* powder and 400 mL of deionized water. The mixture was cooled to room temperature after boiling for 30 min. Thereafter, the mixture was filtered through filter paper. The filtrate was maintained at 4 °C for use in the temperature-controlled synthesis of SNPs.

SNP preparation

About 100 mL of aqueous *Z. spina* leaf extract was mixed in 1.2 g of sodium bisulfate ($Na_2S_2O_3 \cdot 5H_2O$) while the mixture was shaken at room temperature. The sodium bisulphate solution was shaken, and 10% hydrochloric acid was added dropwise to facilitate even sulfur crystallization. Centrifugation was used to concentrate the resultant sulfur suspension particles for 20 min at room temperature and at 1000 rpm. The sediment was cleaned repeatedly with distilled water and absolute ethanol to eliminate any biological material. After removing the upper liquids, the product was vacuum dried at 60 °C for 4 h.

Preparation of a PC solution

The PC solution was prepared by dissolving 8 g of pure PC in 100 mL of chloroform with continuous stirring and using a magnetic stirrer at room temperature (25 °C) for 1 h. A homogeneous solution of pure PC was obtained [14].

Preparation of polymeric films

By dissolving PC with chloroform, samples were prepared in flakes and then catalyzed by adding SNPs. A glass plate with a thickness of 60±5 µm was used for casting. The thickness of polymeric flakes was measured by using a micrometer device (USA, Company, Panel Q, Vtester UQ). The models were cut into slices (1.5×3 cm) for the purpose of conducting measurements.

Sample irradiation

Samples were irradiated with a 356 nm, 18 W UV lamp. The polymer films were placed in a way to ensure that they received the same amount of radiation exposure during the specified irradiation periods.

3. Optical fractionation of PC

The following methods were used for optical polymer film fractionation: UV-Vis method, FT-IR, and viscometry as follows:

UV-Vis spectroscopy

UV-vis device was used to measure the absorbance of polymer films in the 200–700 nm range. Equation (1) was used to calculate Kd (degradation rate constant) resulting from the optical oxidation process of polymeric films:

$$\ln (A_\infty - A_t) = \ln (A_\infty - A_\circ) - K d t \quad \ldots\ldots\ldots(1)$$

Where:

A_o= before irradiation, absorbance of the polymeric films

A_t= at the irradiation time (t), absorbance of the polymeric films themselves.

A_∞= for infinity of time, absorbance of the polymeric films.

A straight line with a slope of (-Kd) was determined by constructing the relationship between ln (At∞–Ao) and irradiation time (t seconds), thereby suggesting the first class of additive degradation.

Infrared spectroscopy

IR spectroscopy was applied to determine the growth rate of the carbonyl group (I_{CO}) by comparing the intensity of the absorbed bands (400–4000 cm^{-1}) before and after irradiation for each duration of pure PC chips with different concentrations of SNPs. An absorption band for the carbonyl group (C=O) at 1765 cm^{-1} was visible in the spectrum, which facilitated the determination of the carbonyl index (I_{CO}) growth factor. Equation (2) was then applied, using the band index method [15, 16]:

$$I_{(s)}=A_{(s)}/A_{(R)} \quad \text{..... (2)}$$

wherethe growth factor of the group under study is represented by $I_{(s)}$, absorbance of the group under study is represented by $A_{(s)}$, and absorbance of the reference peak is represented by $A_{(R)}$.

Measuring of Viscosity

The viscosity method was used to determine the uniformity of molecular weight. The Houwink–Mark equation was applied to determine the partial weight of the polymer wafer based on its viscosity features. The following were used to determine the hash score (α). The same relationships were used to ascertain the numerical average of the series (S) division based on viscosity measurements [17]. The degree of fragmentation (α) was calculated using the following relationship:

$$\boldsymbol{\alpha = \frac{1}{P_t} - \frac{1}{P_\circ}} \qquad \boldsymbol{\dots (3)}$$

The cutting series' numerical rate (S) is as follows:

$$\boldsymbol{S = \alpha\, p_0} \qquad \dots \dots \dots (4)$$

4. RESULTS AND DISCUSSION

Structural properties of SNPs (green method)

FT-IR spectra

Z. spina trees are displayed in Figure (a1). The stretching vibrations of the amino (-NH) and hydroxyl (-OH) groups in alcohols and phenols were responsible for the strong and wide absorption bands observed at 3282 cm^{-1}. The asymmetric stretching vibrations and symmetric stretching vibrations of the $-CH_2$ and $-CH_3$ functional groups in aliphatic compounds were responsible for the absorption peaks at 2919 and 2852 cm^{-1}, respectively. The shoulder peak at 1729 cm^{-1} was associated with the stretching vibrations of carboxyl groups. The carbonyl amide group in the first and second amides distinguished the band at 1619 cm^{-1}. The scissoring vibrations of protein methylene groups accounted for the absorption band at 1443 cm^{-1}. The vibration of the C-N bonds in carboxylic acids and aromatic amines produced a spectral band at 1371 cm^{-1}. The band at 1033 cm^{-1} corresponded to the stretching vibrations of the second carbon atom in alcohols. Aromatic compounds were identified by the peaks at 516 and 559 cm^{-1}. Throughout the synthesis process, these functional groups serve as agents for coating, distributing, and stabilizing SNPs. Figure 2(b) shows the FT-IR spectrum of the SNPs, which revealed the existence of a novel chemical bond on their surface. Thus, the application of seder leaf extract may aid in the dispersion and stability of SNPs. The process of stopping particle agglomeration was achieved by taking advantage of interactions between amino acid residues of the protein and SNPs. FT-IR revealed a prominent peak at 460 cm^{-1}, clearly showing the effect of seder leaf extract on SNPs [18,19].

a)

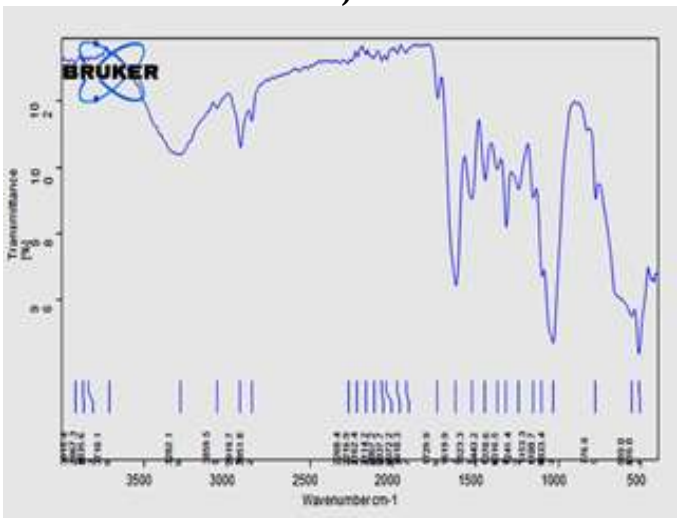

b)

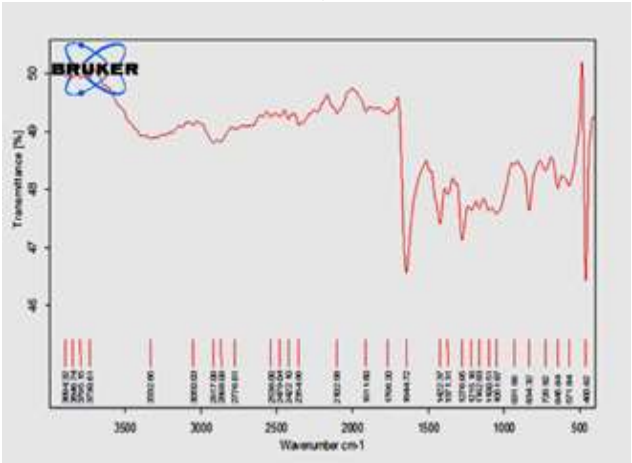

Figure 1: (a) FT-IR analysis of *Ziziphus spina* tree extract. **(b)** FT-IR analysis of synthesized sulfur nanoparticle

SEM measurements

SEM images of SNPs extracted from the leaves of the *Z. spina* tree are represented by Figure (2). These images show how the nanoparticles created with the described method had a nearly spherical shape and

uniform size. The SEM results showed that sulfur crystals agglomerated during processing.

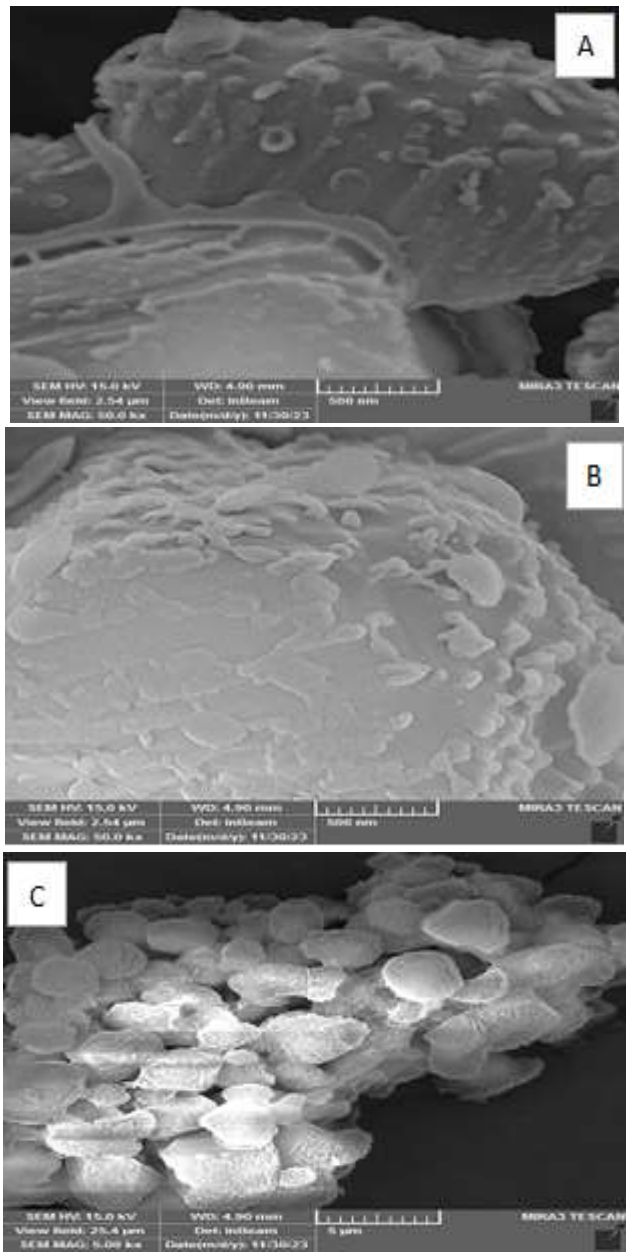

Figure (2): A–C SEM results of the prepared SNPs

XRD measurements

XRD analysis was conducted to determine the crystal structure of the green SNPs produced. After directing X-rays at the sample, the locations of the peaks from different angles were determined. Figure 3 shows the XRD data for SNPs next to the standard sulfur reference pattern (JCPDS 4:8-0247). We found that the corresponding angles (15.260, 22.990, 24.320, 26.310, 27.319, 28.580, 31.089, 42.860, 55.390, and 65.140) were associated with the diffraction peaks (113), (220), (222), (040), (313), (044).), (422), (319), (515), and (266), respectively. The clearly defined crystal structure of the SNPs was demonstrated and confirmed by these data. The Debye–Scherer equation was used to calculate the nanoparticle size [20,21]:

$$D = K \cdot \lambda / \beta \cdot \cos\theta$$

where 9.26 nm is the size of SNPs determined by the Debye–Scherer equation.

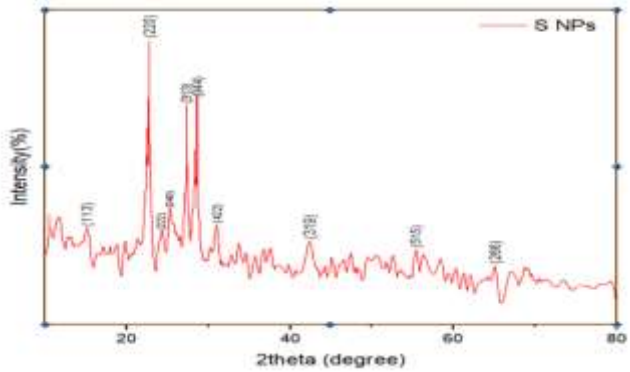

Figure 3: XRD pattern of the prepared sulfur nanoparticles

Optical fractionation of polycarbonate

Optical segmentation of thick (60±5 µm) polymeric films of pure PC that consisted of various concentrations of nanosulfur. The SNPs were monitored to assess the effect of their increase. The concentration of SNPs in relation to polymer dissolution at various irradiation times was analyzed via UV-Vis, FT-IR measurements, and viscometry.

UV spectroscopy

The photodegradation of polymeric films composed of pure PC and those containing different weights of SNPs was determined by UV spectroscopy. When polymeric films were exposed to UV radiation for a particular time, the films underwent yellowing, which indicated the photodegradation of the polymer [22] (Table 1). The absorbance values obtained from UV spectroscopy were utilized to determine the photodissociation rate constant (Kd) at different times after the irradiation process. The absorbance of polymeric films varied with the irradiation period and amount of SNPs added.

Table (1): Absorbance values of pure polycarbonate films.

Chip type	Irradiation time (hours)	Absorbency A_t				
		0,0	30	60	120	180
PC		0.74	0.879	1.229	1.403	1.507
PC + 0.00625 % S		0.809	0.974	1.382	1.523	1.843
PC + 0.0125 % S		0.812	1.150	1.536	1.860	1.986
PC + 0.025 % S		0.816	1.236	1.689	1.99	2.24

PC + 0.05 % S	**0.825**	**1.403**	**1.809**	**2.077**	**2.501**
PC + 0.1 % S	**0.831**	**1.523**	**2.104**	**2.461**	**2.666**

Compared with films of pure polymer, the absorption spectrum of polymer films prepared with 60±5 micron thickness and different additive concentrations varied with the irradiation times. Figures 4–6 illustrate that the absorbency of the membranes increased proportionally with the increase in material concentration due to the presence of effective aggregates. Figures 7–9 show that the photodissociation constant of polymer films in the presence of added nanomaterial was calculated by plotting the relationship between (ln (A∞ - At) and irradiation time. We obtained a straight line, which indicated that optical fragmentation constituted a first-order reaction.

The UV spectroscopic measurements shown in Table 1 indicated that the absorptive values of pure PC film were directly proportional to its irradiation time. The absorption value before irradiation was 0.74, which rose to 1.507 after 180 h of irradiation (Figure 4). The absorbance values for PC films containing different concentrations of nanomaterial increased with increasing additive concentration while maintaining a consistent irradiation time. It possessed higher absorbency than pure polymer. For example, at the radiation time of 60 h, the absorption of pure polymer was 1.229, which increased to 1.536 at the additive concentration of 0.0125%. This increase persisted during absorption, with the concentration of the additive increasing to a maximum of 2.104 at 0.1% for the same irradiation time. This was applicable to the other stages of irradiation. The absorption spectrum of the prepared polymer films with a thickness of 60±5 micrometers and containing different concentrations changed with different irradiation times compared with that of the pure polymer film. The absorption of films increased with the concentration of additive compound due to the increase in effective aggregates. Figure 5 illustrates that films containing 0.0125% of an additive exhibited increased absorption with prolonged irradiation time, and this trend was similarly observed in the highest concentration used of 0.1% (Figure 6).

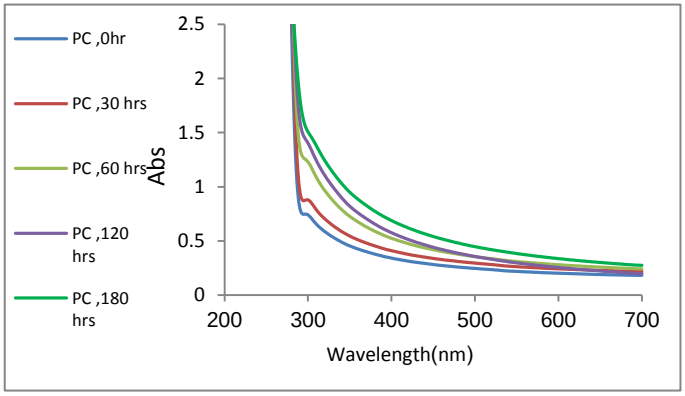

Figure (4): UV-vis spectrum of additive-free polycarbonate films.

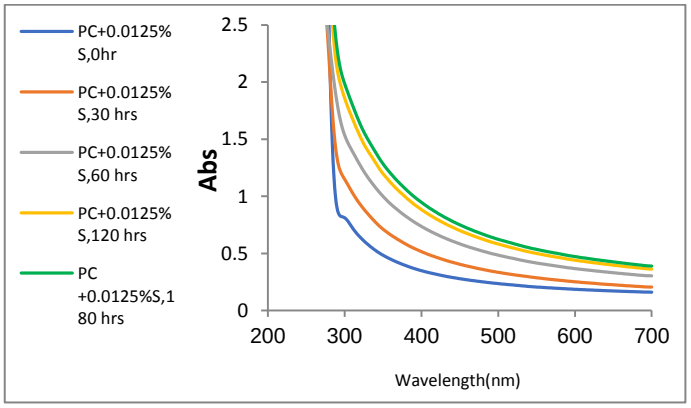

Figure (5): UV-vis spectrum of polycarbonate alcohol films with 0.0125% of nanosulfur.

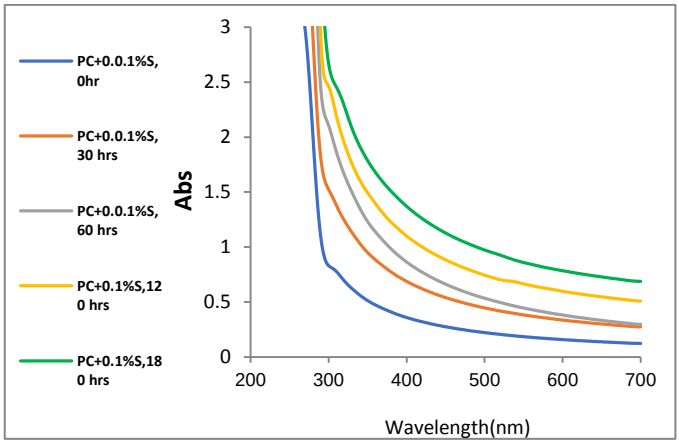

Figure (6): UV-visible spectrum of polycarbonate films with 0.1% of nanosulfur

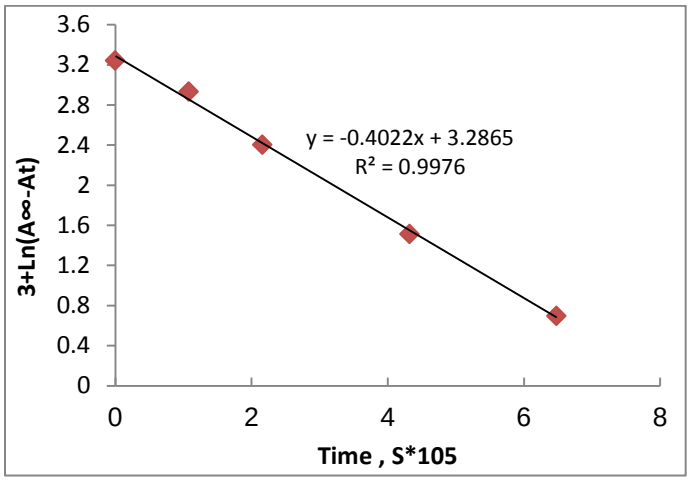

Figure (7): Relationship between natural logarithm of absorbance of nanosulfur at 0.0125% in polycarbonate films and irradiation time

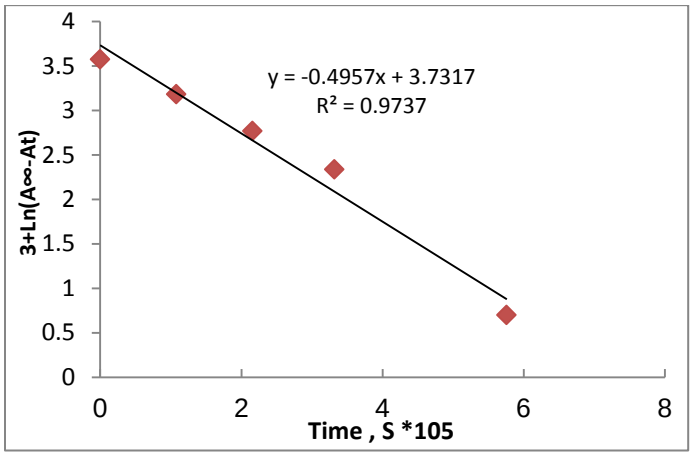

Figure (8): Relationship between natural logarithm of absorbance of nanosulfur at 0.05% in polycarbonate films and irradiation time

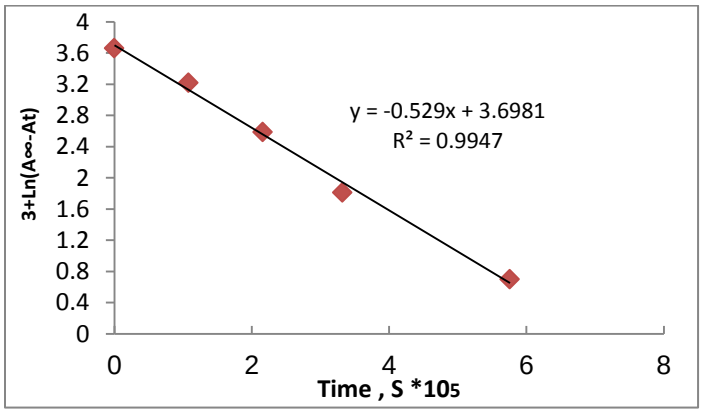

Figure (9): Relationship between natural logarithm of absorbance of nanosulfur at 0.1% in polycarbonate films and the irradiation time.

The slope of the straight line derived from previously mentioned shapes was used to compute the value of Kd (photodissociation speed constant) of nanosulfur added to PC based on the specified concentrations. The data indicated that Kd increased directly with the concentration of nanomaterial added to the polymers, as shown in Table 2. An increase in SNPs enhanced the reaction speed of light with the polymer.

Table (2) Kd' values for nanoscale sulfur (S) in polycarbonate films

Concentration%	K_d (Sec.)$^{-1}$x10^{-5}
PC + 0.00625 % S	0.358
PC + 0.0125 % S	0.402
PC + 0.025 % S	0.440
PC + 0.05 % S	0.495
PC + 0.1 % S	0.529

Infrared spectroscopy

Over numerous irradiation periods, the photodissociation of pure PC films consisting of various percentages of nanosulfur was monitored in the range of 400–4000 cm^{-1} via FT-IR. The absorption bands of the carbonyl (C= O) group, induced by the polymer's interaction with photons in the presence of oxygen, appeared at the frequency of 1765 cm^{-1} [23]. Oxygen functioned as a catalyst, whereas SNPs served as a disintegration catalyst.

The growth of the absorption band was monitored. Given that the maximum value was found under high concentration, the carbonyl group was used to monitor the chemical activity of pure polymer films containing varying concentrations of nanosulfur. Thus, the carbonyl growth coefficient (I_{CO}) was computed via the baseline technique [24].

After exposing pure PC films with a thickness of 60±5 micrometers to FT-IR measurements, a comparison with the pre-irradiation pure PC revealed that the IR characteristics varied with different irradiation times. Figure 10 shows the IR spectrum of pure PC before irradiation. Figure 11 illustrates the FT-IR spectrum of PC after 120 h of irradiation. A change in the scope of the carbonyl group was observed.

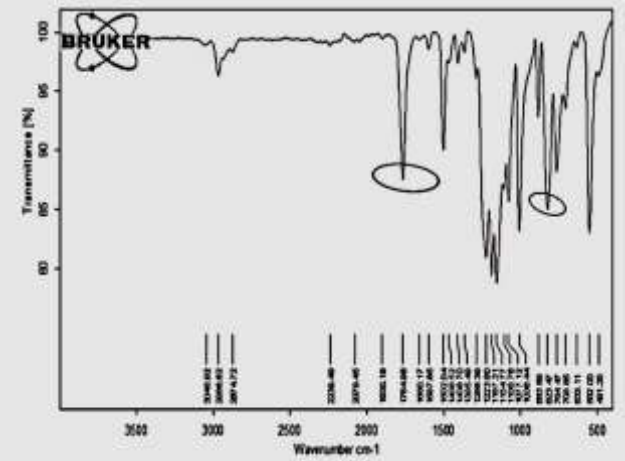

Figure (10): FT-IR of additive-free polycarbonate film before irradiation

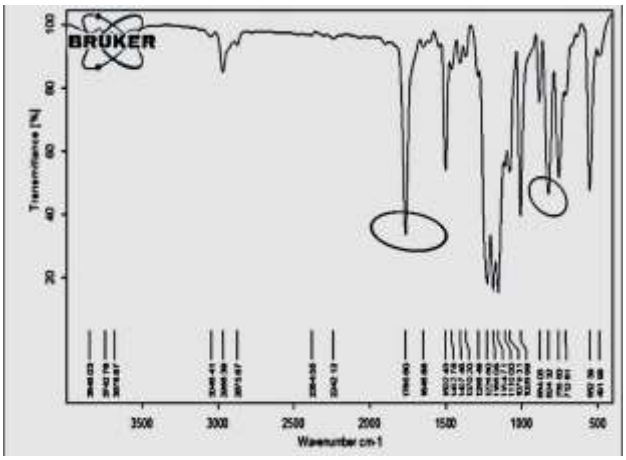

Figure (11): FT-IR of a thin polycarbonate film without additives at an irradiation time of 120 h

Concentration of 0.1% of polycarbonate film with thickness of 60±5 µm SNPs, changing as in Figure (12), after 180 h of irradiation.

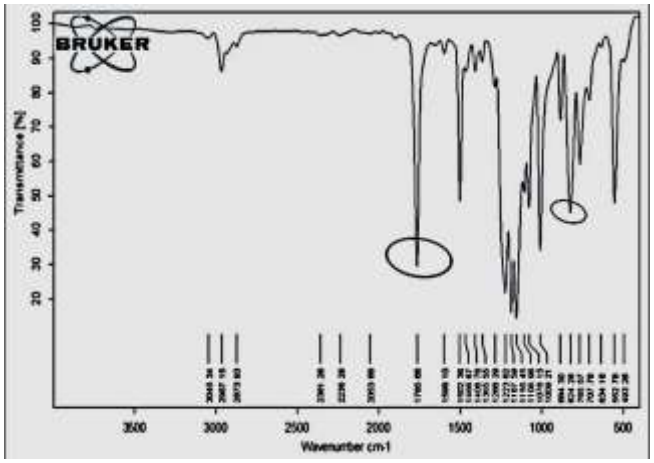

Figure (12): FT-IR analysis of polycarbonate film containing nanosulfur (S) at 0.1% concentration and an irradiation time of 180 h.

The values for the carbonyl group absorption coefficient (I_{CO}) were computed. The pure PC film and the films with various SNP concentrations are indicated in Table 3.

Table (3): I_{CO} with irradiation time for polycarbonates containing various nanosulfur (S) concentrations.

Percentage of additives	I_{CO}				
	0.0	30	60	120	180
PC	1.417	1.506	1.618	1.734	1.875
PC + 0.00625 % S	1.450	1.598	1.720	1.854	1.956
PC + 0.0125 % S	1.456	1.714	1.832	1.964	2. 055
PC + 0.025 % S	1.459	1.820	1.928	2.110	2.156
PC + 0.05 % S	1.461	1.945	2.083	2.186	2.250
PC + 0.1 % S	1.464	2.113	2.220	2.324	2.386

We observed a direct relationship between the value of the carbonyl coefficient (I_{CO}) of pure PC with the irradiation time; the value of the carbonyl coefficient (I_{CO}) increased as the irradiation time increased. The IR spectrum showed that in the case of high concentrations, the carbonyl absorption coefficient (I_{CO}) increased with the increased photodissociation of PC, as shown in Figures 13 and 14. Thus, this nanomaterial was a good fractionation agent.

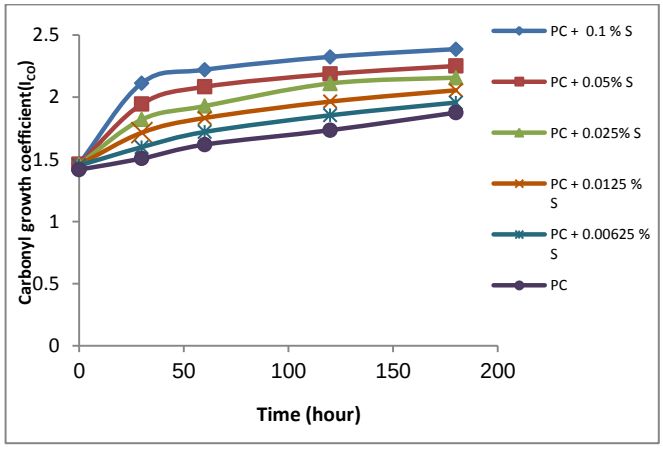

Fig (13): Relationship between I_{CO} and the irradiation time table (3)

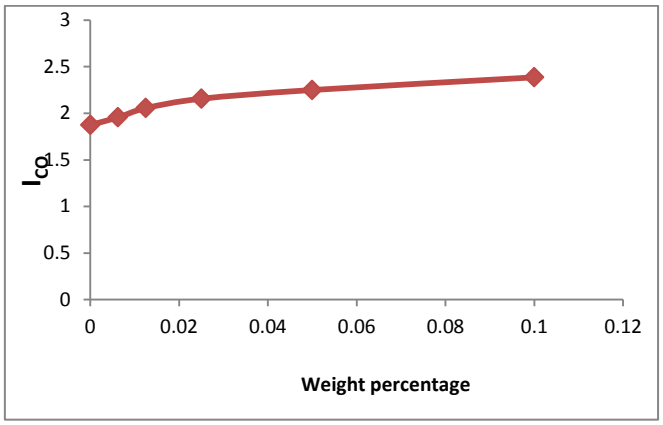

Figure (14): Change in the absorption coefficient of the carbonyl group with the concentration of nanosulfur (S) for polycarbonate sheets over a period of 180 h.

Viscosity measurement

The average molecular weight decreased with increasing irradiation time, as shown in the viscosity measurements, because of the fragmentation of the polymer chain (Tables 4 and 5). Figure 15 shows the decrease in the viscosity molecular weight in the presence of the additive. The molecular weight decreased rapidly at the beginning of irradiation and then it slowed down; this rapid decrease was attributed to the breaking of weak bonds [25]. Figure 16 shows that the speed of decrease in the rate of viscosity molecular weight was directly proportional to the square of the viscosity molecular weight at a specific time [26], and the bonds were distributed randomly along the polymer chain. This was proven through the linear relationship of the rate of chain cutting and the degree of fragmentation in Figures 17 and 18 [27]. This result indicated the efficiency of the nanomaterial in increasing optical fragmentation. Therefore, nanomaterials can be used in large quantities to produce plastics, shopping bags, agricultural containers, and single-use tools to accelerate their breakdown and prevent environmental pollution with plastics. The results of our experimental research were consistent with the information from the references in this field. A previous study indicated that the decomposition of PC is effective in the presence of nickel oxide nanoparticles. This study demonstrated that the molecular weight of the polymer decreased with an increase in the number of hours of irradiation, and the average molecular weight of PC increased with the increase in the addition of nanoparticles on the surface of the polymer [28].

Table (4): Viscosity molecular weight measurements of pure PC flakes

Time Irradiation (hrs.)	$\overline{(M_v)}x10^3$	$(M_v)^2x10^9$	$\frac{dM_v}{dt} = \frac{M_{v0} - M_{vt}}{t}$	Degree of Polymerization P	$\frac{1}{P}x10^{-3}$	Deg. Degree $\alpha\ x\ 10^{-3}$	Ava. Chain Scission (S)
0	188.321	35.464	∞	740.604	1.350	0.0	0.0
30	150.558	22.667	0.349	592.095	1.688	0.338	0.250
60	132.124	17.456	0.260	519.600	1.924	0.574	0.425
120	96.934	9.396	0.211	381.209	2.623	1.273	0.942
180	82.644	6.830	0.163	325.011	3.076	1.726	1.278

Table (5): Viscosity molecular weight measurements of PC chips containing 0.025% nanosulfur (S)

Time Irradiation (hrs.)	$\overline{(M_v)}x10^3$	$(M_v)^2x10^9$	$\frac{dM_v}{dt} = \frac{M_{v0} - M_{vt}}{t}$	Degree of Polymerization P	$\frac{1}{P}x10^{-3}$	Deg. Degree $\alpha\ x\ 10^{-3}$	Ava. Chain Scission (S)
0	188.321	35.464	∞	740.604	1.350	0.0	0.0
30	142.002	20.164	0.428	558.447	1.790	0.440	0.325

60	121.556	14.775	0.309	478.039	2.091	0.741	0.548
120	84.093	7.071	0.241	330.710	3.023	1.673	1.239
180	70.745	5.004	0.181	278.216	3.594	2.244	1.661

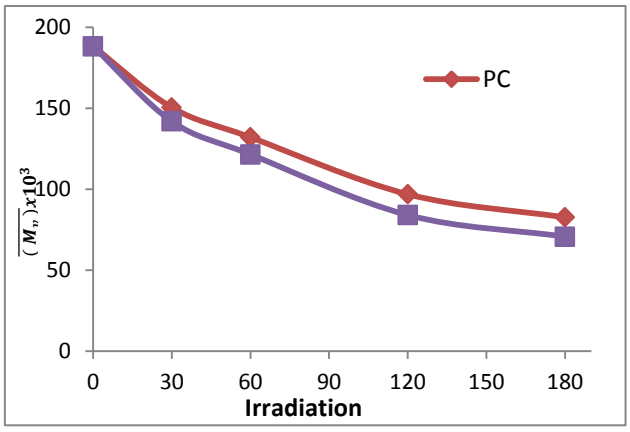

Figure (15): Relationship between the viscosity molecular weight rate and the irradiation time of PC chips with/without 0.025% of nanosulfur (S).

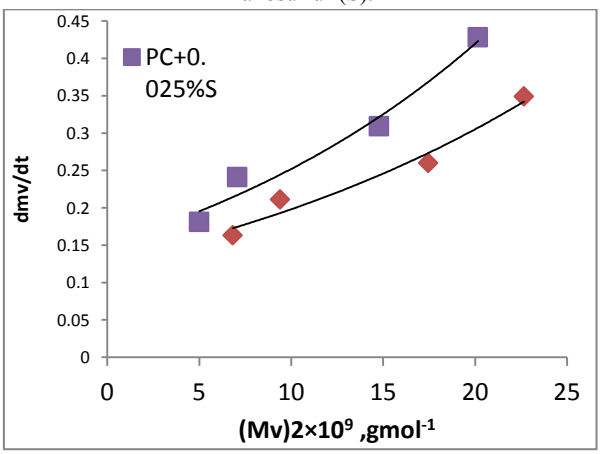

Figure (16): Relationship between dMv/dt and square viscosity molecular weight rate of PC chips with/without 0.025% of nanosulfur (S)

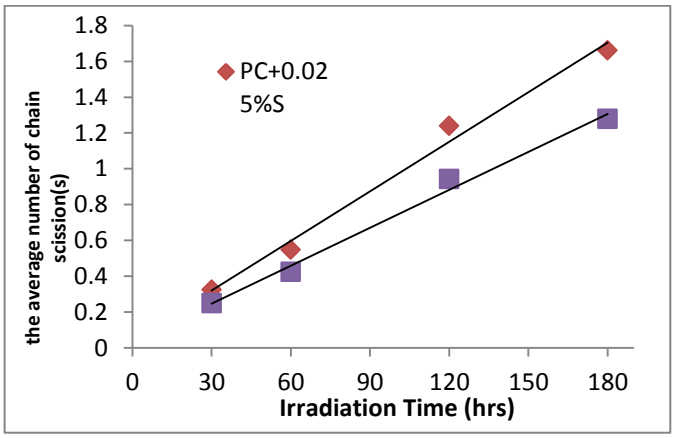

Figure (17): Relationship between numerical rate of chain cutting and the irradiation time of PC chips with/without 0.025% of nanosulfur (S)

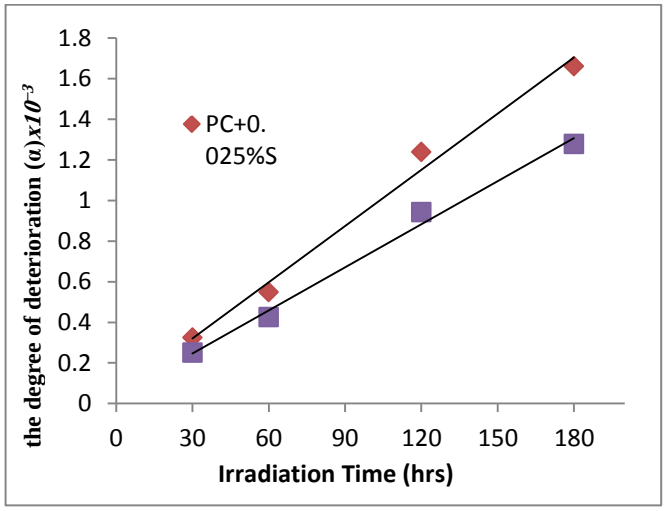

Figure (18): Relationship between degree of fragmentation and irradiation time of PC chips with/without 0.025% of nanosulfur (S)

Conclusions

Using an extract from the leaves of the *Z. spina* tree, SNPs were synthesized. Their synthesis was proven by SEM, FT-IR, and XRD measurements. Several different concentrations of SNPs were mixed with PC polymer, and spectral measurements were conducted. The decomposition of PC was directly proportional of the concentration of the added nanoparticles. The results of the analyses showed that the added material at different percentile concentrations increased the photolytic fragmentation of the polymer flakes compared with the flakes that did not contain additives, which encouraged their use as a catalyst for photolytic degradation. Moreover, PC flakes at high concentrations of SNPs led to a faster degradation process than those at low concentrations. The molecular weight of the polymer

decreased with an increase in the number of irradiation hours, indicating the polymer's decomposition. Furthermore, SNPs were found to increase light absorption. This research examined the photolytic degradation of the polymer to identify new ways for mitigating environmental pollution through photolytic processes.

References

[1] Gadge, G.G.(2020).An Overview: Natural Polymers and their Applications. *Research Journal of Pharmaceutical Dosage Forms and Technology*, *12*(2), 131-136.

[2] Terzopoulou,Z.,Zamboulis,A.,Koumentakou, I., Michailidou, G., Noordam, M. J., & Bikiaris, D. N. (2022). Biocompatible synthetic polymers for tissue engineering purposes. *Biomacromolecules*, *23*(5), 1841-1863.

[3] Jadhav, V. D., Patil, A. J., & Kandasubramanian, B. (2022). Polycarbonate nanocomposites for high impact applications. *Handbook of consumer nanoproducts*, 257-281.

[4] Ang, R. R., Sin, L. T., Bee, S. T., Tee, T. T., Kadhum, A. A. H., Rahmat, A. R., & Wasmi, B. A. (2015). A review of copolymerization of green house gas carbon dioxide and oxiranes to produce polycarbonate. *Journal of Cleaner Production*, *102*, 1-17.

[5] Kyriacos, D. (2017). Polycarbonates. In *Brydson's Plastics Materials* (pp. 457-485). Butterworth-Heinemann.

[6] Al-mhmdy, Y. M., Ali, H. K., & Shihab, O. H. (2023). Induction of Photodegradation of Poly (vinyl alcohol) Using a Cobalt Binary Mixed Ligand Complex. *Journal of University of Anbar for Pure Science*, *17*(2), 115-125.

[7] Sazali, N., Ibrahim, H., Jamaludin, A. S., Mohamed, M. A., Salleh, W. N. W., & Abidin, M. N. Z. (2020, April). Degradation and stability of polymer: A mini review. In *IOP Conference Series: Materials Science and Engineering* (Vol. 788, No. 1, p. 012048). IOP Publishing.

[8] Diepens, M. (2009). Photodegradation and stability of bisphenol a polycarbonate in weathering conditions.

[9] Joshi, H., Choudhary, P., & Mundra, S. L. (2019). Future prospects of nanotechnology in agriculture. *Int. J. Chem. Stud*, *7*(2), 957-963.

[10] Gupta, P. K. (2023). Introduction and Historical Background. In *Nanotoxicology in Nanobiomedicine* (pp. 1-22). Cham: Springer International Publishing.

[11] Attia, T. S., & Elsheery, N. I. (2020). Nanomaterials: scope, applications, and challenges in agriculture and soil reclamation. *Sustainable Agriculture Reviews 41: Nanotechnology for Plant Growth and Development*, 1-39.

[12] Yuan, H., Liu, Q., Guo, Z., Fu, J., Sun, Y., Gu, C., ... & Dhankher, O. P. (2021). Sulfur nanoparticles improved plant growth and reduced mercury toxicity via mitigating the oxidative stress in Brassica napus L. *Journal of Cleaner Production*, *318*, 128589.

[13] Najafi, S., Razavi, S. M., Khoshkam, M., & Asadi, A. (2020). Effects of green synthesis of sulfur nanoparticles from Cinnamomum zeylanicum barks on physiological and biochemical factors of Lettuce (Lactuca sativa). *Physiology and molecular biology of plants*, *26*, 1055-1066.

[14] Odian, G. (2004). *Principles of polymerization*. John Wiley & Sons.

[15] Anju, V. P., & Narayanankutty, S. K. (2017). Impact of Bis-(3-triethoxysilylpropyl) tetrasulphide on the properties of PMMA/Cellulose composite. *Polymer*, *119*, 224-237.

[16] Patnaik, P. (2003). *Handbook of inorganic chemicals* (Vol. 529, pp. 769-771). New York: McGraw-Hill.

[17] Wang, J., Huang, H., & Huang, X. (2016). Molecular weight and the Mark- Houwink relation for ultra- high molecular weight charged polyacrylamide determined using automatic batch mode multi- angle light scattering. *Journal of Applied Polymer Science*, *133*(31).

[18] Al Banna, L. S., Salem, N. M., Jaleel, G. A., & Awwad, A. M. (2020). Green synthesis of sulfur nanoparticles using Rosmarinus officinalis leaves

extract and nematicidal activity against Meloidogyne javanica. *Chemistry International*, *6*(3), 137-143.

[19] M Awwad, A., M Salem, N., & O Abdeen, A. (2015). Noval approach for synthesis sulfur (S-NPs) nanoparticles using Albizia julibrissin fruits extract. *Advanced Materials Letters*, *6*(5), 432-435.

[20] Thakar, M. A., Jha, S. S., Phasinam, K., Manne, R., Qureshi, Y., & Babu, V. H. (2022). X ray diffraction (XRD) analysis and evaluation of antioxidant activity of copper oxide nanoparticles synthesized from leaf extract of Cissus vitiginea. *Materials Today: Proceedings*, *51*, 319-324.

[21] Khairan, K., Aryati, F., Suhayla, P. D., Sriwati, R., & Awang, K. (2023, May). Green synthesis of sulfur nanoparticles using garlic (Allium sativum): Fungicidal activity and plant growth effects on chili plants (Capsicum annum L.). In *AIP Conference Proceedings* (Vol. 2480, No. 1). AIP Publishing.

[22] Tjandraatmadja, G. F., Burn, L. S., & Jollands, M. C. (2002). Evaluation of commercial polycarbonate optical properties after QUV-A radiation—the role of humidity in photodegradation. *Polymer degradation and stability*, *78*(3), 435-448.

[23] Anju, V. P., & Narayanankutty, S. K. (2017). Impact of Bis-(3-triethoxysilylpropyl) tetrasulphide on the properties of PMMA/Cellulose composite. *Polymer*, *119*, 224-237.

[24] ALI, K., & A ABDULRAZAQ, S. A. M. A. R. (2013). INDUCED PHOTO-DEGRADATION OF POLYSTYRENE BY USING NICKEL (II)-COMPLEX (NI-BAP). *Journal of University of Anbar for Pure Science*, *7*(1), 162-175.

[25] Chiantore, O., Camino, G., Costa, L., & Grassie, N. (1981). 'Weak links' in polystyrene. *Polymer Degradation and Stability*, *3*(3), 209-219.

[26] Chandra, R. and Handa, S. P. (1982). J. Appl. Polym. Sci.,p.1945,27.78

[27] Ranby, B., & Rabek, J. F. (1975). Photooxidation, photodegradation and photostabilisation of polymers.

[28] Kareem, B. M. A., & Ali, H. K. (2022). Study of the photolysis of polycarbonates in the presence of the prepared nickel oxide nanoparticles. International Journal of Health Sciences, 6(S8), 4150–4166 https://doi.org/10.53730/ijhs.v6nS8.13125.

تحضير جسيمات الكبريت النانوية ومعرفة تأثيرها على التحلل الضوئي لمتعدد الكاربونات

رند مال الله حسن* حميد خالد علي مثنى محمد سرحان****

* قسم الكيمياء ، كلية التربية للعلوم الصرفة ، جامعة الانبار ، العراق
** قسم الكيمياء ، كلية التربية للعلوم الصرفة ، جامعة الانبار ، العراق

الخلاصة:
تضمنت هذه الدراسة تحضير جسيمات الكبريت النانوية باستخدام مستخلص اوراق Ziziphus-spina وتمت دراسة تأثيرها على التحلل الضوئي لأغشية متعدد الكاربونات بسمك(60±5) ميكرون، بعد اضافة تراكيز مختلفة من المادة النانوية المضافة (0.1%، 0.05%، 0.025%، 0.0125%، 0.00625%) الى محلول متعدد الكاربونات المذاب في الكلوروفورم ، تم تشخيص جزيئات الكبريت النانوية باستخدام تقنيات مختلفة SEM,XRD,FT-IR. تم تحديد حزمة عند 460 سم-1 وفقاً لتحليل الأشعة تحت الحمراء (FT-IR)، مما يشير إلى تكوين جسيمات الكبريت النانوية. وتمت متابعة التحلل الضوئي لمتعدد الكاربونات بوجود وعدم وجود المادة المضافة باستخدام تحليل الاشعة فوق البنفسجية-المرئية باستخدام الضوء وبطول موجي ٣٥٦ نانومتر بأزمان تشعيع مختلفة(0,30,60,120,180) ساعة وذلك بحساب ثابت سرعة التجزئة الضوئية للمادة المضافة البوليمرية ، بينت النتائج انه عند زيادة تركيز المادة النانوية يزداد التحلل الضوئي للرقائق البوليمرية مقارنة مع الرقائق الخالية من المادة المضافة ، وباستخدام تحليل FT-IR تم حساب معامل امتصاص الكاربونيل حيث وجد ان معامل امتصاص الكاربونيل يزداد مع زيادة تركيز الكبريت النانوي المضاف ، وتتوافق هذه النتائج مع قيم ثابت السرعة للتجزئة الضوئية(Kd) ، وكذلك تم استخدام مقياس اللزوجة لحساب معدل الكتلة الجزيئية للبوليمر ، درجة التفكك والمعدل العددي لقطع السلسلة البوليمرية ووجد ان معدل الوزن الجزيئي للبوليمر يقل مع زيادة زمن التشعيع ويزداد معدل قطع السلسلة

الكلمات المفتاحية: متعدد الكاربونات، التحلل الضوئي، نانو، كبريت، بوليمرات.